THE PENNSYLVANIA STATE UNIVERSITY
SCHREYER HONORS COLLEGE

DEPARTMENT OF CHEMISTRY

SIZE EFFECTS ON GOLD NANOPARTICLE ELECTRONIC DENSITY OF STATES

HANNAH PRILLER
FALL 2024

A thesis
submitted in partial fulfillment
of the requirements
for a baccalaureate degree
in Mechanical Engineering and Chemistry
with honors in Chemistry

Reviewed and approved* by the following:

Dr. Benjamin Lear
Professor of Chemistry
Thesis Supervisor

Dr. Stewart Mallory
Assistant Professor of Chemistry & Chemical Engineering
Honors Advisor

Dr. Raymond Schaak
DuPont Professor of Materials Chemistry
Advisor

*Signatures are on file in the Schreyer Honors College and Department of Chemistry.

Abstract

Gold nanoparticles (AuNPs) have varying applications including, but not limited to, plasmonic solar cells, photocatalysis, photothermal heating, cancer treatment, and more. These applications are built on the electronic properties of the nanoparticles, which arise from their electronic structure and which can be controlled by ligand identity, ligand size, size of the particle, and more. The electronic change in these particles continues to be a topic of perennial interest because of their various applications. While much focus has been given to the evolution of the plasmon with size, this is not a direct measure of their electronic structure. We present work in which we use measurements of Pauli paramagnetism to directly probe the change in the density of electronic states with particle size. This is done to characterize where the electronic properties of AuNPs becomes one in the same with bulk gold, which is expected to occur asymptotically. AuNPs were synthesized from gold salt ($HAuCl_4$) and octanethiol. Size was measured with TEM and paramagnetism was measured with Evans method NMR and TGA. Below a diameter of 5 nm, it was concluded that there is no trend between gold nanoparticle diameter and electronic density of states.

Table of Contents

List of Figures

List of Symbols & Abbreviations

AuNPs	Gold nanoparticles
DCM	Dichloromethane
DLVO theory	Derjaguin-Landau-Vervey-Overbeek theory
ICP-MS	Inductively coupled plasma mass spectrometry
NMR	Nuclear Magnetic Resonance
OECT	Organic electrochemical transistors
PEDOT:PSS	poly(3,4-ethylenedioxythiophene):poly(styrenesulfonate)
RBF	Round Bottom Flask
TEM	Transmission Electron Microscopy
TGA	Thermogravimetric Analysis
TOAB	Tetraoctylammonium bromide
UV-Vis	Ultraviolet-Visible

Acknowledgments

I would like to thank my parents, friends, and everyone in the Lear lab for their friendship and support over the last four and half years. My parents have always supported me and my dreams and helped me to push myself in school. My friends have motivated me and encouraged me through difficult times. Finally, everyone in the Lear Lab has taught me so much, not just about chemistry, but also about learning new things and expanding my scope.

Specifically, I would like to thank Dr. Ben Lear for his mentorship and support from day one. He welcomed me in my first semester and has encouraged me the whole way through.

Lastly, I would like to thank the Pennsylvania State University and the NSF Grant 2304821. Additionally, we state that the findings and conclusions do not necessarily reflect the view of the funding agency.

Chapter 1
Introduction

Nanoparticles are small clusters of atoms that can vary in size and have properties that are unique from their bulk counterparts. This difference is what makes them an interesting system to study. Specifically, gold nanoparticles are small clusters of gold atoms surrounded by ligands. They can range in size from just a few nanometers to upwards of 100 nanometers and are visually distinct from bulk gold, often looking dark purple or red while bulk gold is yellow and shiny. Gold nanoparticles have also exhibited catalytic activity whereas bulk gold is often inert and have various applications in places where bulk gold does not. This difference in application is controlled by the properties of nanoparticles, including electronic density of states, size, shape, and surface chemistry.

1.1 Nanoparticle structure

Gold nanoparticles have various applications dependent upon their properties, which are dependent upon the structure of the nanoparticles. Gold nanoparticles have a few easily characterizable physical features such as size, shape, and surface chemistry that lend themselves to the resultant electronic properties like electronic density of states.

1.1.1 Electronic Density of States

The electronic density of states is a measure of the density of molecular orbitals in a system. As more atoms are added, a nanoparticle increases in size and there is an increase in the number of orbitals. Many of these orbitals are degenerate (are at the same energy level), so there is an associated density of orbitals at different energy levels as well as an associated density of orbitals within energy gaps between orbitals (Fig. 1.1).

Electrons fill in these orbitals starting with the lowest energy, with each orbital having

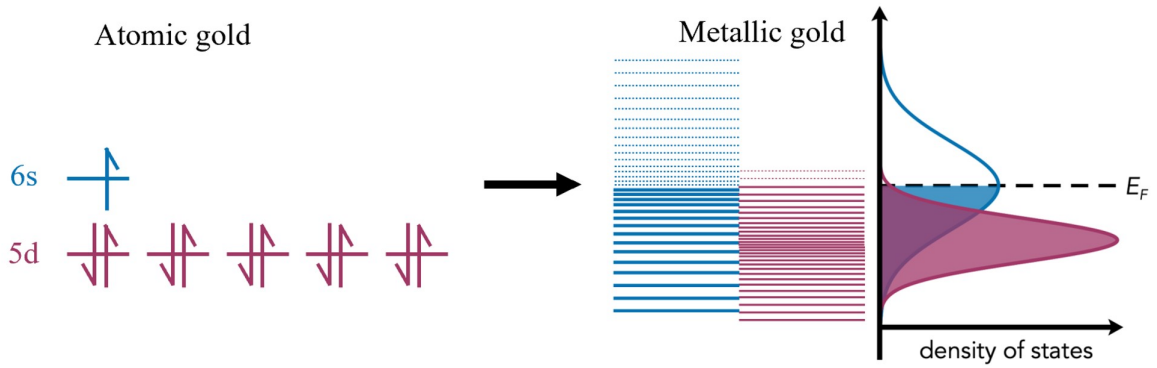

Figure 1.1. Change in orbitals from atomic gold to metallic gold, showing the associated density of states and Fermi energy (E_F).

one spin up electron and one spin down electron. Orbitals are filled until all free electrons have been placed. The energy level at absolute zero of the highest energy orbital that is occupied by an electron is called the Fermi energy. [10] With a change in the size, and therefore the number of orbitals in a nanoparticle system, the density of states at the Fermi energy will change. This can affect different material properties such as electrical and thermal conductivity. Bulk gold contains fully filled $5d$ orbitals and partially filled hybridized $6sp$ orbitals, the latter of which allows gold to act as a conductor. Smaller gold nanoparticles have a gap between their highest occupied and lowest unoccupied molecular orbitals which decreases as the nanoparticle increase in size. [11] A reduction in this gap size improves the electrical conductivity and is just one example of how the density of states at the Fermi energy can affect the properties of gold nanoparticles.

1.1.1.1 Surface Plasmon Resonance

The high electronic density of states at the Fermi energy is also what affects the surface plasmon resonance. When a plasmonic metal is exposed to light, the oscillating electromagnetic field causes the free, conduction electrons to oscillate (Fig. 1.2).

The surface conduction electrons are pushed away from the metal surface but are attracted by the resultant positive charge on the metal. [12] However, when the metal is confined to a smaller size, such as in a nanoparticle, the oscillation of electrons is also confined, and is thus known as local surface plasmon resonance. [13] This oscillation causes a dipole and the amplitude of the oscillation is maximized when the particles are exposed to a specific frequency of light. [14] The specific frequency of light is determined by the boundary conditions of the nanoparticle. When the nanoparticle size becomes comparable to the mean free path of the electrons, the electrons encounter this boundary,

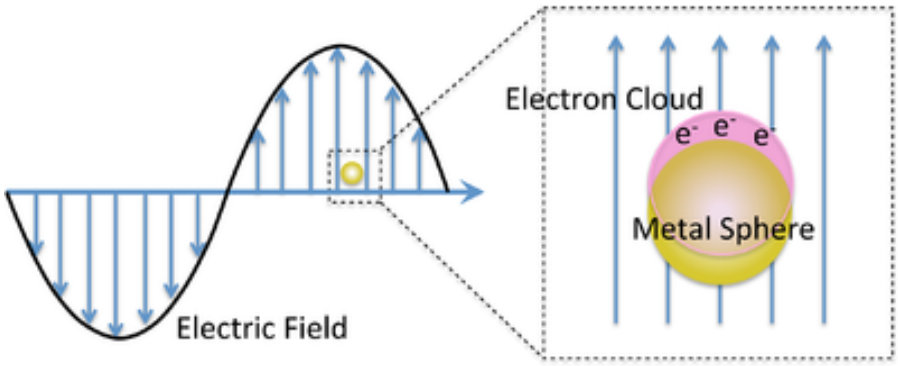

Figure 1.2. Visualization of the localized surface plasmon resonance for a spherical gold nanoparticle. Figure taken from Reference [1].

thus imposing a boundary for which wavelengths of light interact best. [15]

The color of gold nanoparticles, which ranges from dark purple to red and pink, is due to absorption and scattering during surface plasmon resonance as explained by Mie theory. Smaller nanoparticles around 20 nm mainly experience absorption while larger particles around 80 nm experience both absorption and scattering. As gold nanoparticles increase in size, scattering begins to play a larger effect. This is why larger gold nanoparticles are often used for imaging purposes and smaller gold nanoparticles are often used for photothermal therapy. When absorption is the main effect, light is converted into heat which can be used for cell destruction. [14]

1.1.2 Defining Features of a Nanoparticle

Nanoparticles are defined by several physical features, but the most common ones include size, shape, and surface chemistry.

1.1.2.1 Size

The size of a nanoparticle is often dependent upon the method used for synthesis. One factor that affects size that can be changed during synthesis is the reducing agent. Specifically, the strength of the reducing agent can change the rate of reduction, with stronger reducing agents increasing the reaction rate and decreasing the diameter of the nanoparticle. [16] The concentration of the reducing agent or ligand, such as citric acid in the Turkevich method, can also affect the resulting nanoparticle diameter.

The synthesis of gold nanoparticles using the Turkevich method begins with the reduction of gold and the nucleation of particles. From there, two mechanisms are proposed for how the gold forms spherical nanoparticles. [2] The first method proposes

that the gold initially forms nanowires in solution, which eventually coalesce and cleave into spheres that are capped by citrate (Fig. 1.3).

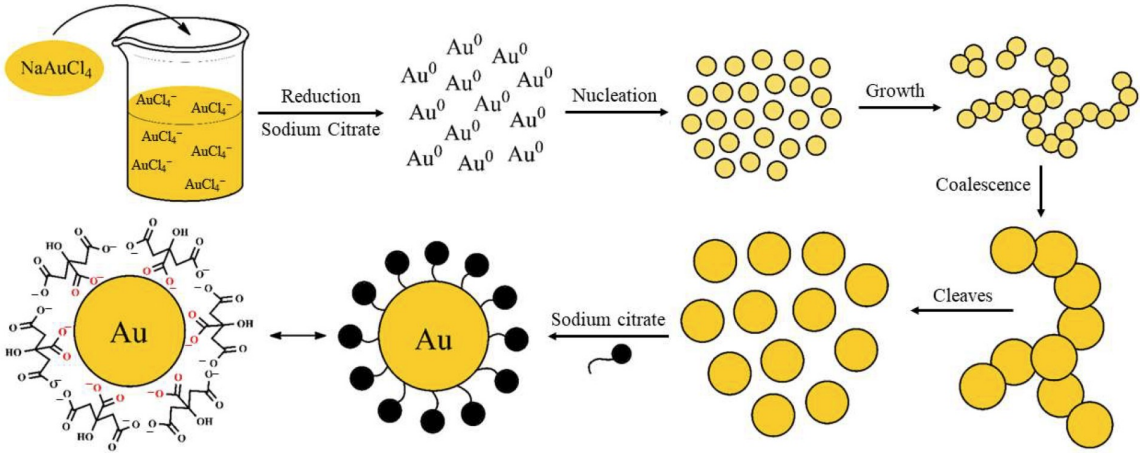

Figure 1.3. Proposed mechanism for spherical gold nanoparticle synthesis through the formation and cleavage of gold nanowires. Figure taken from Reference [2].

The second proposed mechanism is that after nucleation, the gold does not form nanowires and instead grows directly into a sphere (Fig. 1.4).

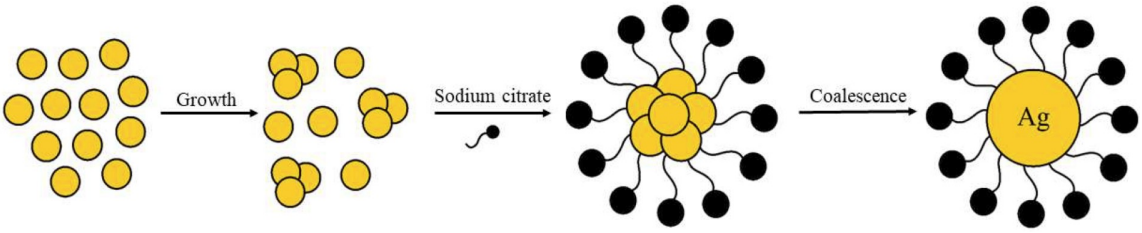

Figure 1.4. Proposed mechanism for spherical gold nanoparticle synthesis without the formation of an intermediary nanowire. Figure taken from Reference [2].

While the exact mechanism for spherical nanoparticle formation in the Turkevich method is still under debate, what is known is that the gold undergoes the general steps of reduction, nucleation, and growth. During reduction, Au^{3+} is first reduced to Au^{+} by the citrate, releasing chloride ions into solution (Reaction 1 in Figure 1.5(1)). The Au^{+} is then reduced again by itself, producing Au^{0} (Reaction 2 in Figure 1.5). This gives an overall reduction reaction of Reaction 3 in Figure 1.5. [2]

After reduction, nuclei (clusters of gold atoms) are formed. Studies done by Polte et al. determined that after nucleation, these nuclei do not continue to grow into larger particles, but coalesce with each other to form the nanoparticles. [17]

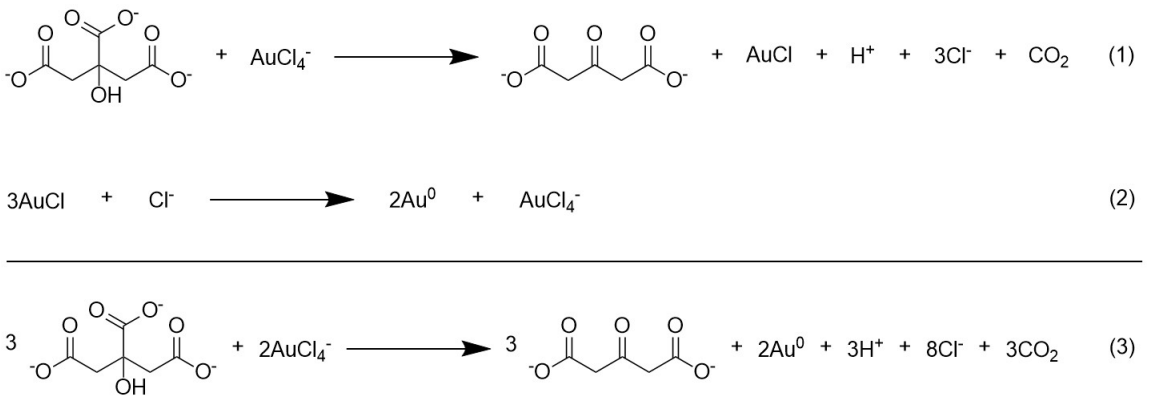

Figure 1.5. Reduction reactions of gold salt to metallic gold. (1) Reduction of Au^{3+} to Au^{+} by citrate. (2) Reduction of Au^{+} to Au^{0}. (3) Overall reduction reaction. [2]

1.1.2.2 Shape

Gold nanoparticles are commonly spherical, but they can also be synthesized into cubes, rods, stars, tetrahedra, and more. Different shapes of gold nanoparticles are often desired because they affect the boundary conditions for localized surface plasmon resonance and are typically anisotropic in this respect. For example, gold nanorods and nanoshells find use in biological applications because they bring the localized surface plasmon resonance from the visible range into the near-infrared range. [18] This shift is caused by the difference in the dimensions for the nanorod, which causes the plasmon to split into two. Additionally, structures like nanorods have enhanced electric fields at their tips, which changes how they scatter light. [19] As spheroid particles become less spherical, their extinction spectra shift. Along the major (longer) axis of the particle, the peak in the spectrum redshifts (Fig. 1.6) while the peak along the minor (shorter) axis blueshifts. Additionally, if the particle is changed along a third axis, there becomes a third plasmon resonance as well. [3]

Gold nanocubes find application in areas such as fundamental optics and plasmon-enhanced spectroscopy. This is due to an enhanced localized electromagnetic field at their edges and corners. [20] Lee and Yoon synthesized nanocube-nanosphere dimers that had interacting plasmons for the purpose of improving surface-enhanced Raman spectroscopy, which is a spectroscopic technique that enhances the light scattering of molecules through plasmon excitation in nanoparticles. [21] [22] Lee and Yoon's UV-Vis extinction spectra revealed two resonance bands for their dimers at 564 nm and 790 nm, while the initial nanospheres had a band at 534 nm and the initial nanocubes had a band at 581 nm. These new bands for the dimer were a result of the coupling of the

plasmons across the longitudinal and the transverse dimensions. Using these dimers for surface-enhanced Raman spectroscopy, the authors found an enhancement factor of $(1.2 \pm 0.2) * 10^{10}$, which is significantly larger than enhancement factors for other nanoassembly structures studied. [21]

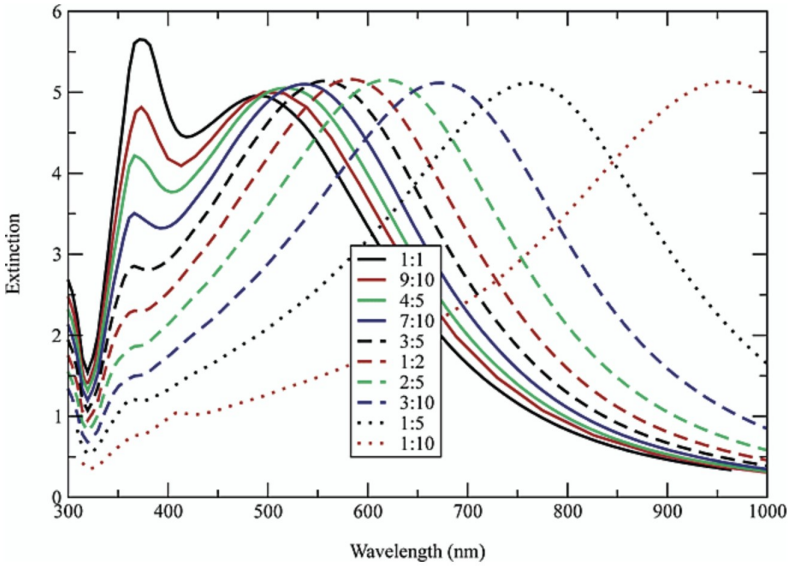

Figure 1.6. Calculated extinction spectra of spheroid particles with different minor axis to major axis ratios. Figure taken from Reference [3].

1.1.2.3 Surface Chemistry

In order to stabilize gold nanoparticles, they often need to be capped by a ligand, or they will otherwise aggregate, thus ceasing to be useful nanoparticles. There is a wide variety of ligands that can be used including thiols, citrates, polymers, and more. In addition to varying the ligand itself, the solvent-ligand interaction can be varied, affecting the solubility and stability of the nanoparticles. Previous work by our lab has studied the relationship between ligand size and electronic density of states. It was found that changing the length of an alkanethiol ligand changes the magnetic susceptibility of the nanoparticle and that the Pauli paramagnetism is inversely proportional to the ligand length. This is due to the longer chain increasing electron donating strength, thereby increasing the level of the Fermi energy to a level with a lower density of states (Fig. 1.7). [4] Other work from our lab has focused on changing the ligand density on alkanethiol-protected gold nanoparticles and found that an increase in surface ligand density results in a decrease in the density of states at the Fermi level. This is due to

an increase in ligand density increasing the electron donation from the ligand, thereby raising the Fermi energy to a level with a lower density of states [23]

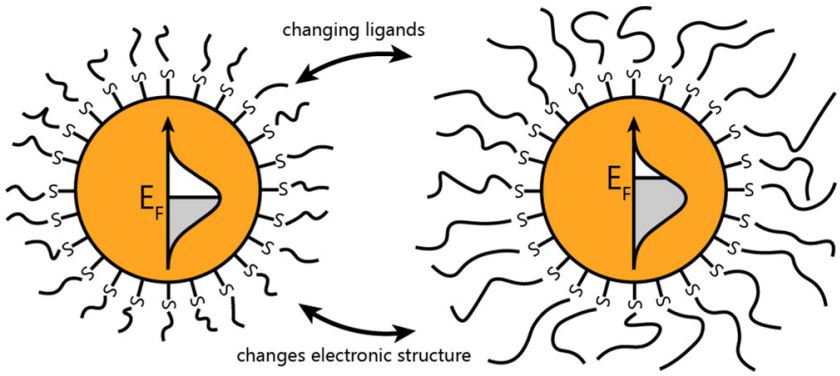

Figure 1.7. Length of alkanethiol ligand chain decreases the electronic density of states at the Fermi energy. Figure taken from Reference [4].

Ligands present during synthesis can also control the size and shape of nanoparticles and are what keep the metal from continuing to grow past the nanoparticle size. This is necessary to keep the nanoparticle properties over time and use them in various applications. [24] A study of gold nanoparticle ligand exchange from citrate to benzyl mercaptan ions saw an increase in particle size due to aggregation (Fig. 1.8).

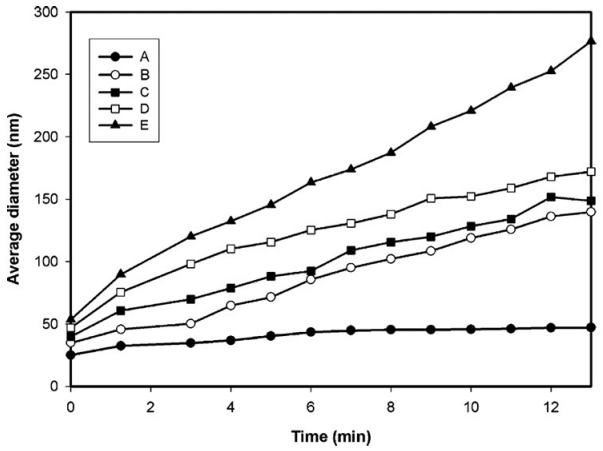

Figure 1.8. Average diameter of nanoparticle increase over time after addition of benzyl mercaptan ions for ligand exchange. Figure taken from Reference [5].

The authors suggested that this size increase was caused by destabilization of the particles from the benzyl mercaptan ions and rationalized this theoretically with the Derjaguin-Landau-Vervey-Overbeek (DLVO) theory. [5] DLVO theory describes the stability of colloidal solutions through the balance of electrostatic repulsive forces and

attractive van der Waals forces. [25] They suggest that controlling the surface potential of nanoparticle systems is an important factor in controlling their stability. [5]

1.2 Nanoparticle Applications

The wide range of features in a nanoparticle is what allows for their application in many different fields. By studying how the electronic properties of a nanoparticle are affected by these various features, specific features can be chosen for their application. Some specific examples of applications include but are not limited to: microelectronics, catalysis, and drug delivery.

1.2.1 Microelectronics

Microelectronics benefit greatly from the ability to change gold nanoparticle properties to tune the desired effects. One such instance of this is in nanoparticle-based transistors. Transistors control the flow of electric current by acting as a switch and are often used in logic circuits. A specific class of transistors is organic electrochemical transistors (OECT), which are often used in detecting various analytes in chemical and biological solutions. Zhang et al. doped a poly(3,4-ethylenedioxythiophene):poly(styrenesulfonate) (PEDOT:PSS) OECT with gold nanoparticles and saw an increase in transconductance by a factor of about 8 (Fig. 1.9). [6] Transconductance is a measure of how much an OECT can amplify a voltage signal. [26] This improvement in the transconductance allowed the authors to use the OECT to detect glucose in a concentration range of 10 nm - 1 mM. This improvement was due to how the gold nanoparticles were annealed to the OECT. Plasmonic heating (heating resulting from plasmon resonance) was used, which allowed for the effective annealing of gold nanoparticles to the PEDOT:PSS film because of the localization of intense heat. [6]

Gold nanoparticles can also be used in photodetectors because of their interaction with visible light. One specific example saw the improvement of ZnO ultraviolet photodetectors after being coated with gold nanoparticles. ZnO microrods are subject to material defects that cause them to emit green light (497-570 nm), which lowers the sensitivity and response speed of the photodetector. However, gold nanoparticles are known to absorb light and have a maximum surface plasmon resonance in this region. After being coated with 2 nm and 5 nm gold nanoparticles, the ZnO microrods saw an increase in on-off current ratios from 2.0 to 4.6 and 4.4, respectively. [27] On-off current ratio is an

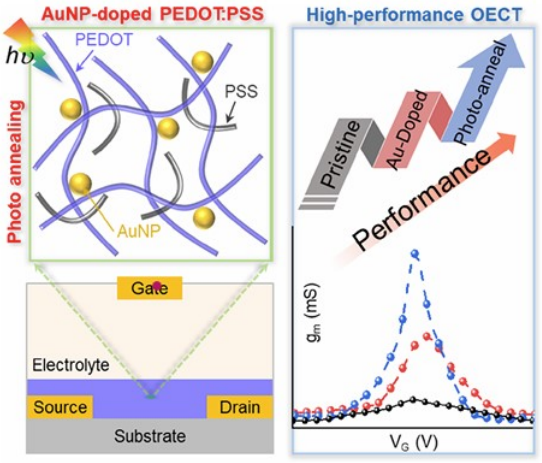

Figure 1.9. Gold nanoparticle doped PEDOT:PSS OECT and comparison of performance to pristine PEDOT:PSS. Figure taken from Reference [6].

important factor in electronic memory and can be affected by the density of states of the material. [28] The ZnO microrods experienced an increase in on-off current ratio with the addition of gold nanoparticles, but saw a decrease in this value as the size of the nanoparticles increased because the nanoparticles began to block more light from reaching the ZnO. [27] This decrease could also be caused by the shift in the localized surface plasmon resonance frequency as a function of size and highlights the need to be able to control nanoparticle size and other properties.

1.2.2 Catalysis

While gold is not known to be particularly reactive, gold nanoparticles have use in catalysis. One study, performed by Sufyan et al., has shown that gold nanoparticles with triphenylphosphine (TPP) or triphenylmethyl mercaptan (TPMT) ligands can be used to catalyze benzyl alcohol oxidation and CO oxidation. During oxidation of CO, the gold surface acts as an adsorption site for oxygen. [29] One model for this mechanism is that the oxygen adsorbs directly on the gold particle and cleavage of the bond is induced by the formation of a four-centered surface complex. [30] Sufyan et al. proved that the electronics of the stabilizing ligand on the gold nanoparticle had an effect on its catalytic ability. The available binding sights on the surface of the gold nanoparticles were measured through titration with 2-Naphthalenethiol, a fluorescent molecule, and showed that both TPP and TPMT coated nanoparticles had similar numbers of binding sites. This rules out that a difference in catalytic activity could be due to availability of surface binding sites. Both the TPP and the TPMT showed similar catalytic activity for

oxidation reactions, but had different catalytic abilities for the reduction of resazurin. The TPP protected nanoparticles were catalytically active while the TPMT protected nanoparticles were not. This is likely because TPP is an electron-donating ligand while TPMT is an electron-withdrawing ligand. This work by Sufyan et al. shows that the electronic properties of the gold nanoparticles can be tuned for catalytic activity. [29]

Gold nanoparticles can also participate in catalysis without the presence of a ligand. Instead, they are bound to the surface of a metal oxide. Figure 1.10 shows a plausible catalytic reaction mechanism for the oxidation of an alcohol. The oxygen first deprotonates through either binding to the gold or the metal oxide. Next, the β-hydride is eliminated and the hydride binds to the gold. This step is proven possible and explained by the presence of positively charged gold atoms in the nanoparticle that are able to accept the hydride. Finally, to complete the catalytic cycle, the reaction is performed in the presence of oxygen that removes the hydride from the gold. The catalytic activity of the gold nanoparticle-metal oxide system depends on the identity of the metal oxide used because they can change how the oxygen interacts with the gold. For example, CeO_2 directly interacts with the oxygen because it is a reducible metal oxide while nonreducible metal oxides are thought to activate the oxygen on the gold nanoparticle. [7]

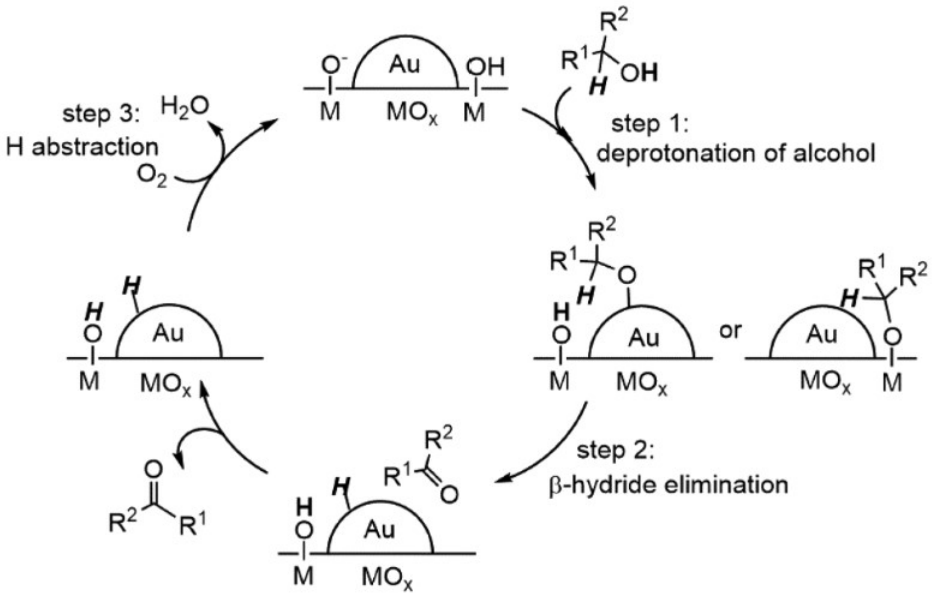

Figure 1.10. Proposed catalytic cycle for oxidation of an alcohol using gold nanoparticles bound to a metal oxide. Figure taken from Reference [7].

1.2.3 Drug Delivery

Gold nanoparticles are often considered for biomedical applications, including drug delivery, because of their tunability, functionalization, biocompatibility and nontoxicity, and their surface electronics. The most notable use of gold nanoparticles in drug delivery is in research focused on cancer therapy. One example is the combination of 30 nm gold nanoparticles with doxorubicin. The two were combined with a pH-sensitive linker that allowed for the release of the doxorubicin inside of acidic organelles (Fig. 1.11). This causes a fast increase in the concentration of the drug to improve the effects inside of tumor cells. Other studies have used polyethylene glycol between the drug and the gold nanoparticle to improve the cytotoxicity and other properties of the drug system. The wide study of gold nanoparticles in this field is tied to the ease of synthesizing differing shapes, sizes, and surface ligands to tune how the system reacts in drug delivery. [31]

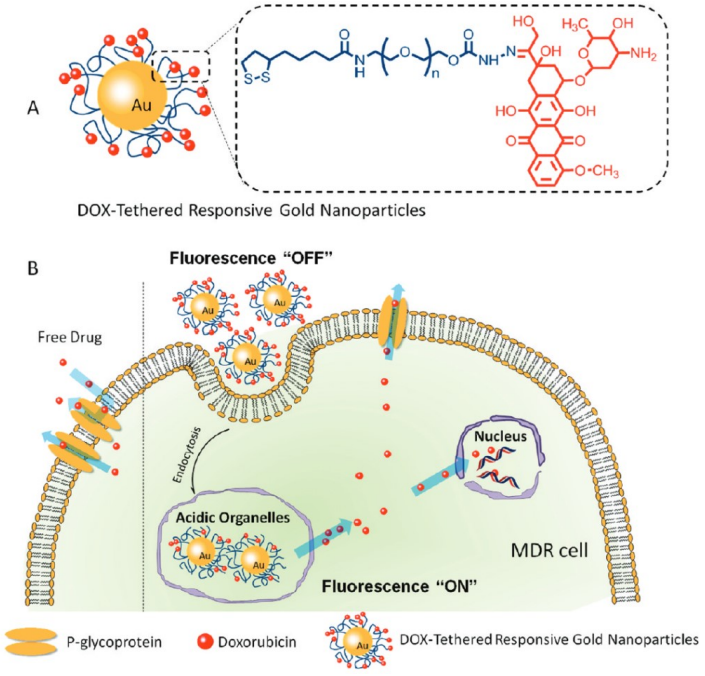

Figure 1.11. (A) Gold nanoparticle coated in linkers with doxorubicin. (B) Illustration of gold nanoparticle entry and release of doxorubicin once inside acidic organelles. Figure taken from Reference [8].

Gold nanoparticles delivering drugs can also be activated through external means such as ultrasound or laser exposure. These methods are based on the local surface plasmon resonance of gold nanoparticles. The heating of gold nanoparticles through plasmon resonance can cause the degradation of heat-sensitive linkers between the gold

nanoparticle and drug, thus releasing the drug only where irradiated. Pulsed lasers and ultrasound reduce the effect of thermal damage due to long exposure and work by gold nanoparticle absorption of light, which forms microbubbles of water vapor around the nanoparticle. The bursting of these bubbles creates mechanical forces that help to open the cell membrane to allow the nanoparticle through. These processes can be visualized in Figure 1.12. [9]

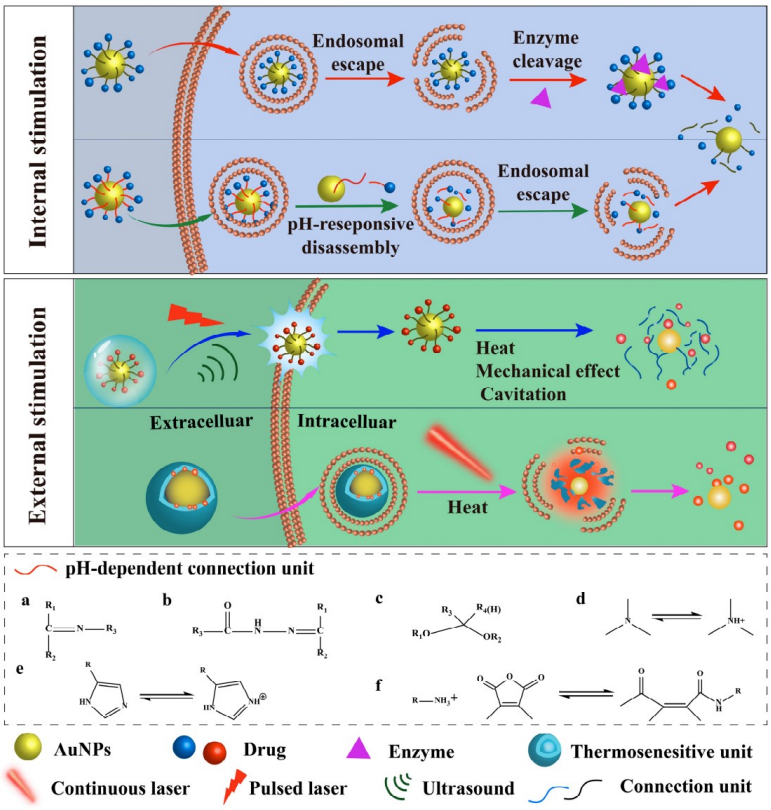

Figure 1.12. Illustration of drug delivery with gold nanoparticles via pH and enzymatic methods (top) and laser and ultrasound methods (bottom). Figure taken from Reference [9].

1.3 Summary of Thesis Work

The goal of this work is to characterize the effect of gold nanoparticle size on the electronic density of states. Knowing this relationship, gold nanoparticles can be used more effectively for various applications. This relationship was characterized by synthesizing gold nanoparticles of different sizes, imaging them with TEM to analyze the size, taking NMR using Evans method to measure the magnetic susceptibility, and using TGA to find the mass ratio of gold to ligand in order to calculate the density of states.

Chapter 2
Synthetic and Characterization Methods

2.1 Synthetic Methods

Gold nanoparticles typically range in size from a few nanometers up to about 200 nm. Synthetic methods typically only make nanoparticles in a certain range of sizes, so two different synthetic methods were used.

2.1.1 Brust-Schiffrin Method

The Brust-Schiffrin method makes gold nanoparticles up to about 5 nm in diameter (Fig. 2.1).

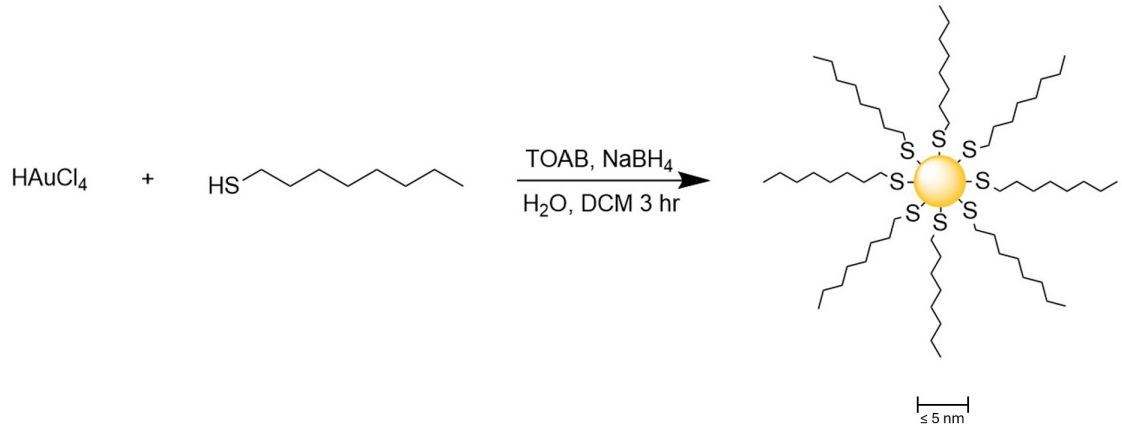

Figure 2.1. Synthesis of octanethiol-protected gold nanoparticles.

This method involves the reduction of gold from the gold salt $HAuCl_4$. It uses $NaBH_4$ as the reducing agent and TOAB as the phase transfer agent. [16] Octanethiol was used as the ligand of choice, since alkanethiols are common stabilizing agents for colloidal gold in organic solutions. [32] Gold nanoparticles resulting from this method are typically an almost black, purple color. The size of the nanoparticles synthesized with this method was controlled by changing the ratio of the concentration of the gold salt to the octanethiol, which a larger amount of octanethiol resulting in a smaller nanoparticle size.

2.1.2 Turkevich Method

The Turkevich method makes gold nanoparticles from 20-200 nm (Fig. 2.2).

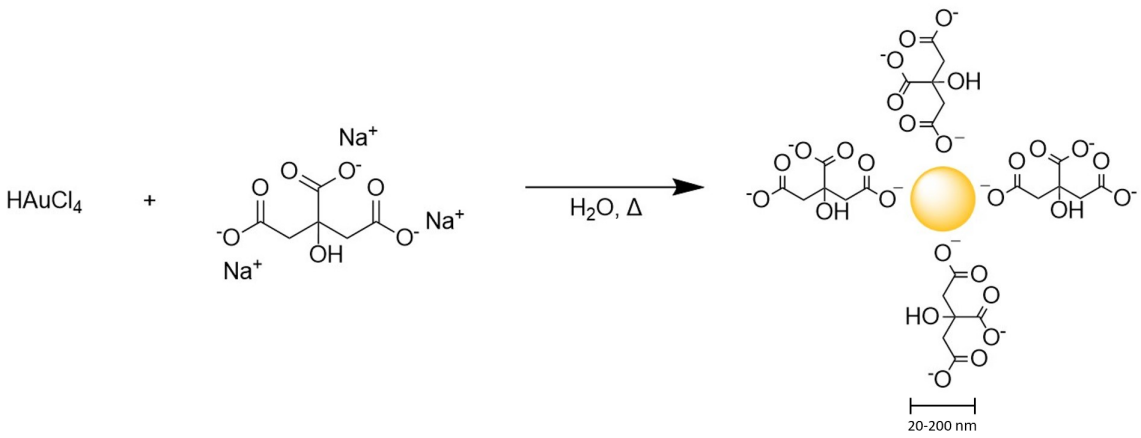

Figure 2.2. Synthesis of citrate-protected gold nanoparticles.

This method involves the reduction of the same gold salt $HAuCl_4$. The reducing agent, sodium citrate, is also the capping agent. [33] Gold nanoparticle solutions resulting from this method are typically a wine-colored dark red or pink. The size of the nanoparticles synthesized with this method was also controlled by changing the ratio of the concentration of the gold salt to the sodium citrate.

2.1.2.1 Ligand Exchange

In order to keep the ligands consistent among particles, the sodium citrate had to be exchanged for octanethiol. Initial attempts to exchange the ligands resulted in the gold being stuck at the interface between the aqueous and organic solvents (Fig. 2.3).

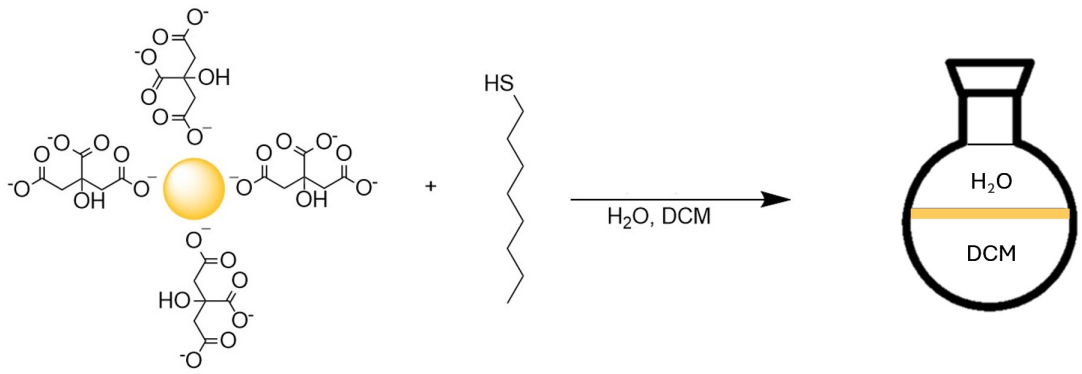

Figure 2.3. Gold nanoparticles being stuck at the interface between the organic and aqueous layers.

It was thought that this was due to an issue with charge compatibility, and so tetraphenylborate was added to allow the nanoparticles to transition into the organic phase. This resulted in the gold leaving the interface and transitioning into the organic phase to make octanethiol-protected larger nanoparticles. This was visually confirmed by the color change of the organic phase from colorless to wine-red (Fig. 2.4).

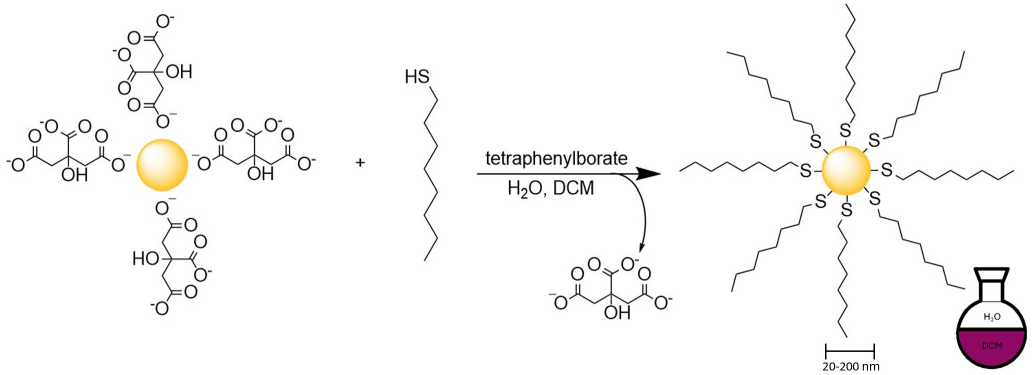

Figure 2.4. Successful ligand exchange of citrate to octanethiol.

2.2 Characterization Methods

2.2.1 Evans Method NMR

To measure the magnetic susceptibility of the nanoparticles, Evans method NMR was used. NMR is capable of measuring this value because of the distribution of electrons with different spin states (Fig. 2.5).

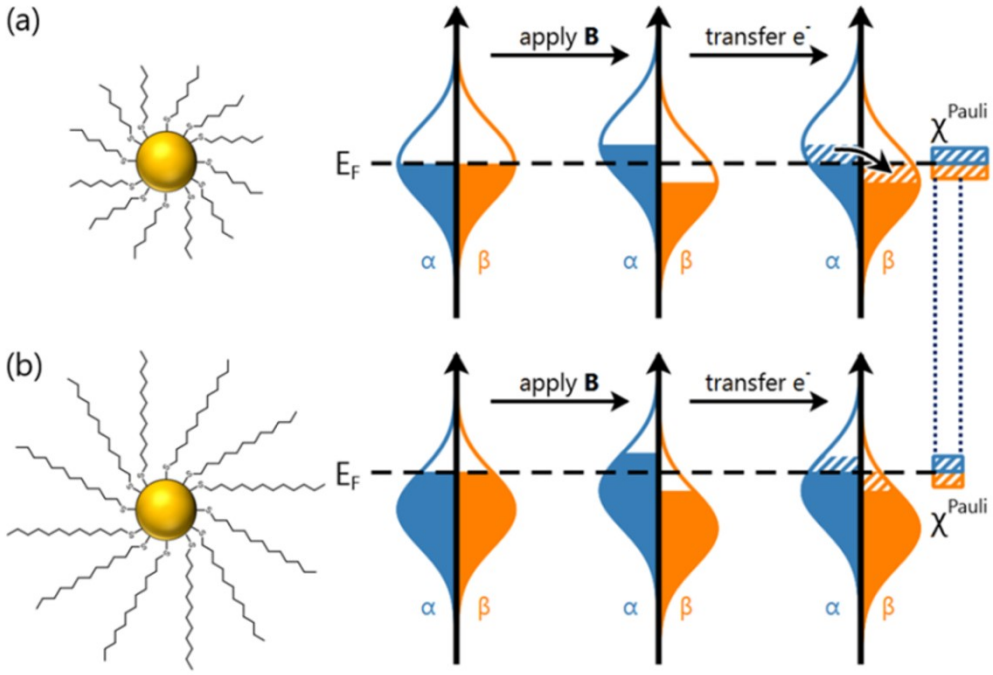

Figure 2.5. Example of how ligand length can affect the electronic density of states. [4]

When a sample is placed in a magnetic field, the electrons in the alpha spin state are raised in energy, while the electrons in the beta spin state are lowered in energy. To keep a constant Fermi energy, some of the electrons in the alpha spin state transition into the beta spin state. This causes a net magnetic moment, the magnitude of which varies depending on the density of states. This magnetic moment is also known as the Pauli paramagnetism and can be related to the magnetic susceptibility of a sample, which is directly measured with Evans method NMR.

Evans method NMR involves the use of an outer and an inner NMR tube. Initially, each NMR tube contains a different solvent and a typical solvent spectrum can be taken (Fig. 2.6a). In this case, CDCl3 and n-hexane were used.

Next, the nanoparticles are added to the n-hexane and a new spectrum is taken (Fig. 2.6b). The addition of the nanoparticles causes the n-hexane peak to shift, and this shift can be measured between the two spectra as in Figure 2.6c. This shift value is then used to calculate the Pauli paramagnetism and the density of states, and this calculation will be discussed in more detail in Chapter 3. [4]

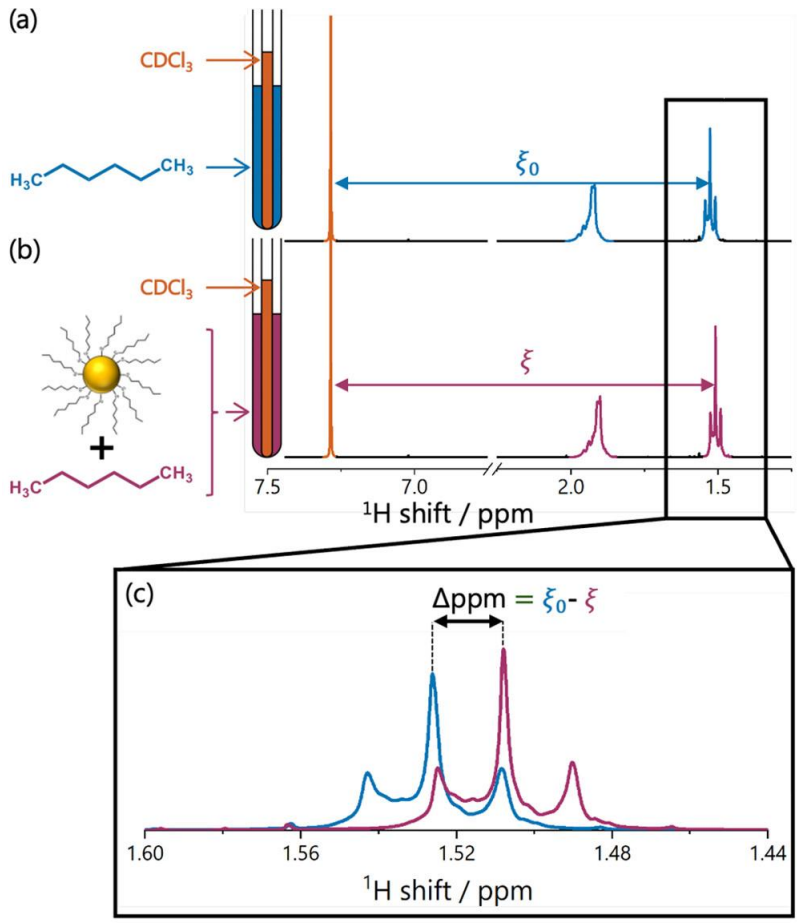

Figure 2.6. An illustration of Evans method NMR. (a) Solvent NMR spectrum. (b) NMR spectrum with nanoparticles. (c) Difference in chemical shift between the two spectra. [4]

2.2.2 TEM

To measure the diameter of the gold nanoparticles, TEM was used to image each set of particles. An example of some of these images can be seen in Figure 2.7.

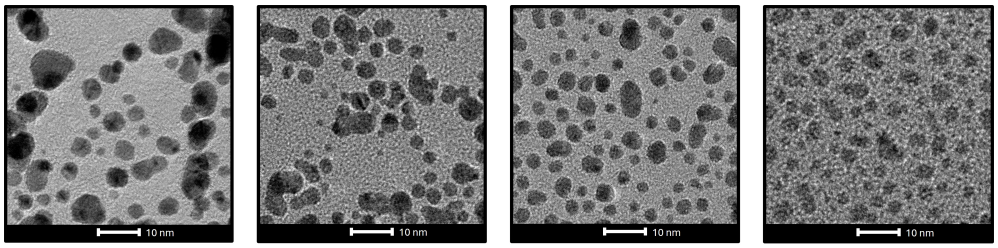

Figure 2.7. Images of different size gold nanoparticles using TEM.

The image processing software ImageJ was used to measure particle size within several images of the same set of particles. A filter was used in the software to make the

nanoparticles black and the background white. (Fig. 2.8)

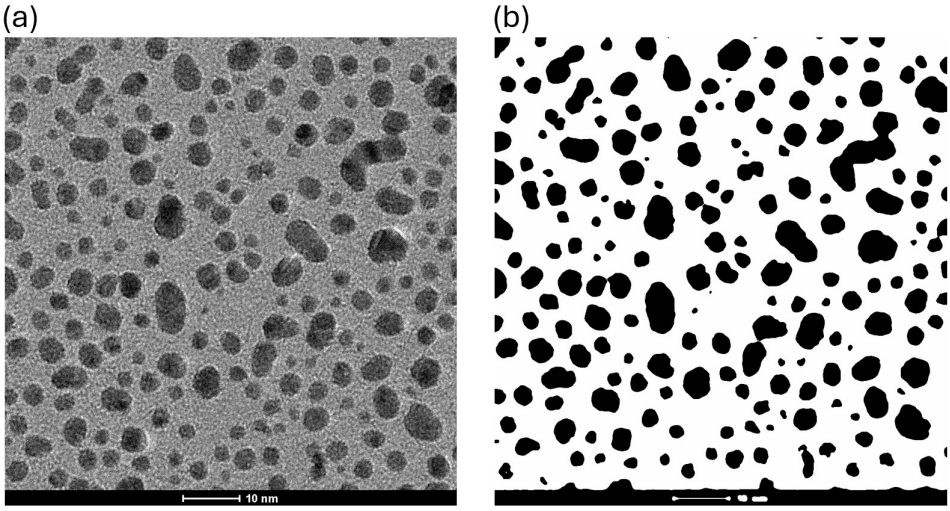

Figure 2.8. (a) TEM of gold nanoparticles and (b) black and white filtered image

The area of each particle in the image was found and the diameter was calculated, assuming that the particles were spherical and ignoring particles along the edge (including the scale bar). A log-normal average was taken to account for larger and smaller particles and overlapping particles in the images (Fig. 2.9).

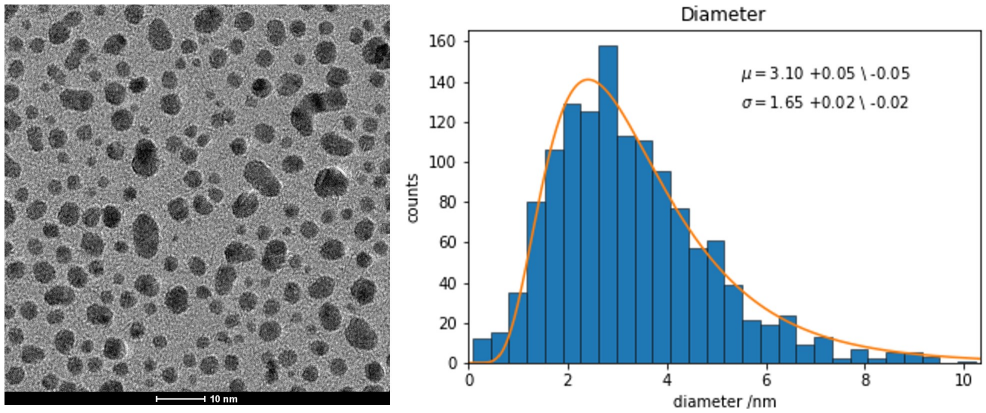

Figure 2.9. TEM image and associated histogram with log-normal fit for the same set of nanoparticles.

2.2.3 TGA

To convert the value for magnetic susceptibility to the value for Pauli paramagnetism, the mass of the gold core and the mass of the ligand shell need to be known. This ratio

is easily found through the use of TGA, which burns off the octanethiol, measuring the mass loss. Since the gold will not burn off, the mass loss measured by the TGA is the mass of the ligand. Knowing the total mass of the sample added, the mass of the gold can also be found.

Chapter 3
Determining the Correlation between Size and Density of States

3.1 Calculation of Density of States

Measured from the NMR spectrum using Evans method is the solvent peak shift (Fig. 2.6c), which can be related to the observed magnetic susceptibility of the sample using Equation (3.1). The observed magnetic susceptibility is proportional to the solvent peak shift, the mass fraction of nanoparticles in the solvent, and the frequency of the NMR used.

$$\chi_{obs} = \frac{3(\xi_0 - \xi)}{4\pi c f} \tag{3.1}$$

$$\begin{aligned} \chi_{obs} &: Observed\ magnetic\ susceptibility \\ \xi_0 - \xi &: Solvent\ peak\ shift \\ c &: Mass\ concentration\ of\ NPs \\ f &: NMR\ frequency \end{aligned}$$

The observed magnetic susceptibility is comprised of 5 different values that each come from a different aspect of the nanoparticle solution (Eq. (3.2)). The Pauli paramagnetism is used in Equation (3.3) to find the electronic density of states. The Landau moment is caused by the induced moment from the ring current of mobile electrons in the NMR. The core electrons of the nanoparticle contribute a diamagnetic moment to the system while the shell contributes a moment due to the presence of the ligands. Finally, the

solvent also contributes a moment to the system that is subtracted out.

$$\chi_{obs} = \chi_{Pauli} + \chi_{Landau} + \chi_{Core} + \chi_{Shell} - \chi_{Solvent} \tag{3.2}$$

$$\begin{aligned}
\chi_{Pauli} &: Pauli\ paramagnetism \\
\chi_{Landau} &: Induced\ moment\ from\ ring\ current\ of\ mobile\ electrons \\
\chi_{Core} &: Moment\ from\ core\ electrons \\
\chi_{Shell} &: Moment\ due\ to\ ligands \\
\chi_{Solvent} &: Moment\ due\ to\ solvents
\end{aligned}$$

The moment contributed from the solvent can be found in literature. [34] The contribution from the core electrons and the shell of the nanoparticle can be calculated using the mass of each from the TGA measurement and values from literature. [34] [35] The Landau contribution can be put in terms of the Pauli paramagnetism, so Equation (3.2) can then be solved for the Pauli paramagnetism, which is used to calculate the electronic density of states (Eq. (3.3)). The electronic density of states is directly proportional to the Pauli paramagnetism, with the constants of proportionality being the permeability of free space and the Bohr magneton. [4]

$$\chi_{obs} = \mu_0(\mu_B)^2 g(E_F) \tag{3.3}$$

$$\begin{aligned}
\mu_0 &: permeability\ of\ free\ space \\
\mu_B &: Bohr\ magneton \\
g(E_F) &: DOS\ at\ the\ Fermi\ level
\end{aligned}$$

3.2 Results

Combining the diameter data from the TEM images and the calculations for density of states, Figure 3.1 can be produced.

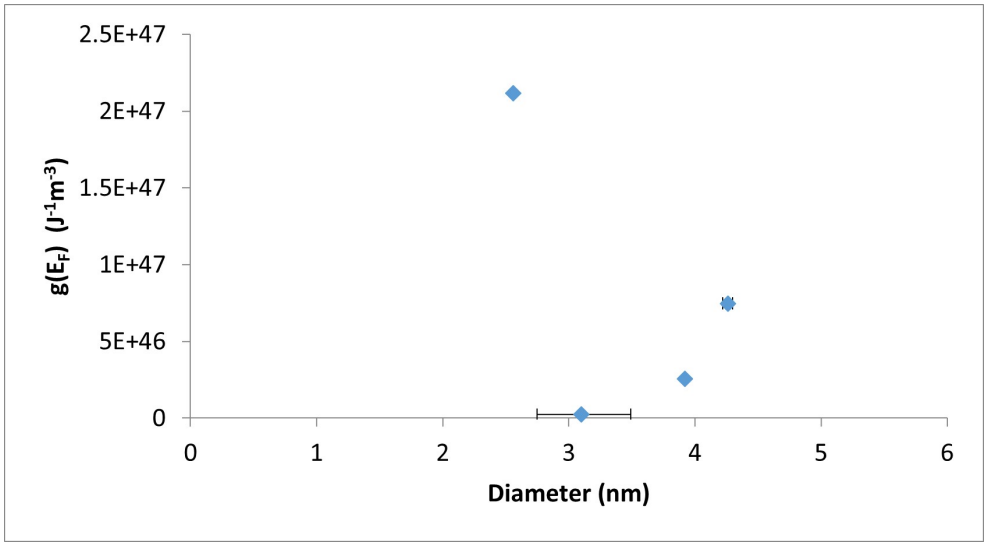

Figure 3.1. Plot of octanethiol-protected gold nanoparticles' electronic density of states with respect to nanoparticle diameter.

While a trend potentially seems to be forming at a diameter of greater than 3 nm, it cannot conclusively be said that there is a trend. Larger nanoparticles have been synthesized with the Turkevich method and are continuing to be worked up to add more data points to Figure 3.1. The data point at 2.56 nm appears to be an outlier, likely because the paramagnetic and diamagnetic contributions have counteracted each other, which is why the χ_{obs} for this set of nanoparticles was 0. We therefore state that at a diameter of less than 5 nm, there is no discernible trend in the electronic density of states with respect to gold nanoparticle diameter.

While current data suggest no trend at a diameter of less than 5 nm, a trend is expected to develop with the addition of larger particles to the data set. Current results indicate an increase in density of states with size past a diameter of 3 nm and it is expected that the electronic density of states will asymptotically approach that of bulk gold. Assuming that this tendency continues, until the electronic density of states reaches the value of bulk gold, it should appear to increase with diameter and then eventually decrease. This would be expected to follow the Gaussian curve for density of states.

Chapter 4
Future Directions

4.1 Electronic Density of States for Larger Gold Nanoparticles

To add data points to Figure 3.1, sets of larger nanoparticles have been synthesized and need to be worked up. These nanoparticles have been synthesized with the Turkevich method and tentatively range in size from 20 nm to 200 nm. The continued work up of these larger particles involves imaging with TEM and size analysis with ImageJ, mass ratio analysis with ICP-MS, and measuring the solvent peak shift with Evans method NMR. A trend will likely be observed that shows the asymptotic approach of the density of states towards the value for bulk gold as the diameter of the nanoparticles increases.

4.2 Use of Different Metallic Cores

While gold is one of the more common metals used for plasmonic nanoparticles, silver is also frequently used and other metals that can be used to synthesize plasmonic nanoparticles include aluminum, copper, palladium, and platinum. [24] These nanoparticles find similar applications in biological, chemical, and other fields because of their plasmonic properties. [36] Once the relationship between gold nanoparticle size and electronic density of states has been developed, this study can be completed for other metallic nanoparticles to observe whether these systems follow the same trend.

4.3 Ligand Exchange Effect on Nanoparticle Size

During the ligand exchange from citrate to octanethiol, it is unknown whether the size of the gold nanoparticles changes. To study whether the ligand exchange affects the nanoparticles' size, the nanoparticles can be imaged with TEM before and after ligand exchange. It is expected that the diameter of the particles increases slightly, as this effect has already been seen in ligand exchanges from citrate to benzyl mercaptan. [5] Documenting this change will allow for method development for the synthesis or larger, thiol-capped gold nanoparticles.

Appendix A
Supporting Information

A.1 Synthetic Methods

A.1.1 Brust-Schiffrin Method

Dissolve 0.1800 g of $HAuCl_4$ in 30 mL of H_2O. Dissolve 1.1 g of TOAB in 20 mL of toluene in a 250 mL RBF and set to stir. Add the $HAuCl_4$ solution to the TOAB solution. Add 0.15 mL of octanethiol. Dissolve 0.1800 g of $NaBH_4$ in 12.5 mL of H_2O and add drop-wise. Allow to stir vigorously for 3 hours. Remove the aqueous layer and add 250 mL of methanol and place in a refrigerator overnight.

Nanoparticle size can be varied by varying the ratio of $HAuCl_4$ to octanethiol.

A.1.2 Nanoparticle Washing

Vacuum filter out the nanoparticles with a fritted filter and remove them from the filter with toluene. Centrifuge the nanoparticle solution at 10,000 rpm for 15 minutes or until the nanoparticles separate from the solution. Decant the solution. Repeat the centrifuging and decanting steps twice more. Use toluene to transfer nanoparticles into vials. For storage, evaporate the solvent and store in a freezer.

A.1.3 Turkevich Method

Dissolve 0.100 g of sodium citrate in 150 mL of H_2O and stir and reflux at 85 °C. Create a 12.5 mL solution of 25 mM $HAuCl_4$ and add drop-wise to the sodium citrate solution. Let the solution stir and reflux for 15 minutes. Store solution in a refrigerator.

Nanoparticle size can be varied by varying the ratio of $HAuCl_4$ to sodium citrate.

A.1.4 Ligand Exchange

Dissolve 0.1 mL of octanethiol in 50 mL of DCM and add to the citrate-protected nanoparticle solution and let stir for at least 30 minutes. Add 0.330 g of sodium tetraphenylborate and allow to stir for at least 30 minutes. Wash nanoparticles according to the washing procedure using DCM.

A.2 Nanoparticle Characterization

A.2.1 Evans Method

Add n-hexane to the outer NMR tube and $CDCl_3$ to the inner NMR tube to take the regular solvent peak NMR. Add a known mass of gold nanoparticles (about 0.0010 - 0.0020 g) to 0.5 mL of n-hexane and add to an outer NMR tube and use an inner NMR tube with $CDCl_3$ to take the nanoparticle NMR.

A.2.2 Thermogravimetric Analysis

Add a known mass of gold nanoparticles to a TGA pan and heat the sample at a rate of 20 °C/minute to 400 °C over a time of 20 minutes. Measure the percent mass loss to obtain the ligand and gold core masses.

A.2.3 Transmission Electron Microscopy

Create a dilute solution of gold nanoparticles using n-hexane (such as the solution used for NMR) and add two drops to a TEM grid. Allow the grid to dry then take TEM images. Using ImageJ, set the scale bar then use an FFT bandpass filter to filter out particles large than 200 pixels and smaller than 20 pixels. Make this image binary (black and white) then analyze the particles to find the area, excluding particles on the edge of the image.

Bibliography

[1] Wikibooks (2021), "Introduction to Inorganic Chemistry". URL: https://en.wikibooks.org/wiki/Introduction_to_Inorganic_Chemistry/Basic_Science_of_Nanomaterials.

[2] Oliveira, A. E. F., A. C. Pereira, M. A. C. Resende, and L. F. Ferreira (2023) "Gold Nanoparticles: A Didactic Step-by-Step of the Synthesis Using the Turkevich Method, Mechanisms, and Characterizations," *Analytica*, **4**(2), pp. 250–263.

[3] Kelly, K. L., E. Coronado, L. L. Zhao, and G. C. Schatz (2003) "The Optical Properties of Metal Nanoparticles: The Influence of Size, Shape, and Dielectric Environment," *The Journal of Physical Chemistry B*, **107**(3), pp. 668–677.

[4] Litak, N. P., L. M. Mawby, and B. J. Lear (2022) "Surface Chemistry Controls the Density of States in Metallic Nanoparticles," *ACS Nano*, **16**(3), pp. 4479–4486.

[5] Kim, T., K. Lee, M. Gong, and S. W. Joo (2005) "Control of Gold Nanoparticle Aggregates by Manipulation of Interparticle Interaction," *Langmuir*, **21**(21), pp. 9524–9528.

[6] Zhang, L., L. Wang, S. He, C. Zhu, Z. Gong, Y. Zhang, J. Wang, L. Yu, K. Gao, X. Kang, and et al. (2023) "High-Performance Organic Electrochemical Transistor Based on Photo-annealed Plasmonic Gold Nanoparticle-Doped PEDOT:PSS," *Applied Materials Interfaces*, **15**(2), pp. 3224–3234.

[7] Ishida, T., T. Murayama, A. Taketoshi, and M. Haruta (2020) "Importance of Size and Contact Structure of Gold Nanoparticles for the Genesis of Unique Catalytic Processes," *Chemical Reviews*, **120**(2), pp. 464–525.

[8] Wang, F., Y. C. Wang, S. Dou, M. H. Xiong, T. M. Sun, and J. Wang (2011) "Doxorubicin-Tethered Responsive Gold Nanoparticles Facilitate Intracellular Drug Delivery for Overcoming Multidrug Resistance in Cancer Cells," *ACS Nano*, **5**(5), pp. 3679–3692.

[9] Huang, H., R. Liu, J. Yang, J. Dai, S. Fan, J. Pi, Y. Wei, and X. Guo (2023) "Gold Nanoparticles: Construction for Drug Delivery and Application in Cancer Immunotherapy," *Pharmaceutics*, **15**(7).

[10] Plieth, W. (2008) *Electrochemistry for Materials Science*, Elsevier.

[11] Rhoden, Z. (2023) *Surface Chemsitry Characterization and Control of the Electronic Structure of Gold Nanosystems*, Ph.D. thesis, The Pennsylvania State Univeristy.

[12] Messersmith, R. E., G. J. Nusz, and S. M. Reed (2013) "Using the Localized Surface Plasmon Resonance of Gold Nanoparticles to Monitor Lipid Membrane Assembly and Protein Binding," *Journal of Physical Chemistry C: Nanomaterials and Interfaces*, **117**(50), p. 26725–26733.

[13] Mayer, K. M. and J. H. Hafner (2011) "Localized Surface Plasmon Resonance Sensors," *Chemical Reviews*, **111**(6), pp. 3828–3857.

[14] Huang, X. and M. A. El-Sayed (2010) "Gold nanoparticles: Optical properties and implementations in cancer diagnosis and photothermal therapy," *Journal of Advanced Research*, **1**(1), pp. 13–28.

[15] Link, S. and M. A. El-Sayed (1999) "Size and Temperature Dependence of the Plasmon Absorption of Colloidal Gold Nanoparticles," *The Journal of Physical Chemistry B*, **103**(21), pp. 4212–4217.

[16] Slepička, P., N. S. Kasálková, J. Siegel, Z. Kolská, and V. Švorčík (2019) "Methods of Gold and Silver Nanoparticles Preparation," *Materials*, **13**(1).

[17] Polte, J., R. Erler, A. F. Thunemann, S. Sokolov, T. T. Ahner, K. Rademann, F. Emmerling, and R. Krahnert (2010) "Nucleation and Growth of GoldNanoparticles Studied via in situ Small Angle X-ray Scattering at Millisecond Time Resolution," *ACS Nano*, **4**(2), pp. 1076–1082.

[18] Agrawal, A., I. Kriegel, and D. J. Milliron (2015) "Shape-Dependent Field Enhancement and Plasmon Resonance of Oxide Nanocrystals," *The Journal of Physical Chemistry C*, **119**(11), pp. 6227–6238.

[19] Murphy, C. J., T. K. Sau, A. M. Gole, C. J. Orendorff, J. Gao, L. Gou, S. E. Hunyadi, and T. Li (2005) "Anisotropic Metal Nanoparticles: Synthesis, Assembly, and Optical Applications," *The Journal of Physical Chemistry B*, **109**(29), pp. 13857–13870.

[20] Park, J. E., Y. Lee, and J. M. Name (2018) "Precisely Shaped, Uniformly Formed Gold Nanocubes with Ultrahigh Reproducibility in Single-Particle Scattering and Surface Enhanced Raman Scattering," *Nano Letters*, **18**(10), pp. 6475–6482.

[21] Lee, D. and S. Yoon (2015) "Gold NanocubeNanosphere Dimers: Preparation, Plasmon Coupling, and Surface-Enhanced Raman Scattering," *The Journal of Physical Chemistry C*, **119**(14), pp. 7873–7882.

[22] Langer, J., D. Jimenez de Aberasturi, J. Aizpurua, R. A. Alvarez-Puebla, B. Auguie, J. J. Baumber, G. C. Bazan, S. E. J. Bell, A. Boisen, A. G. Brolo, and et al. (2020) "Present and Future of Surface-Enhanced Raman Scattering," *ACS Nano*, **14**(1), pp. 28–117.

[23] Haidet, J. (2024) "Impacts of Surface Ligand Coverage on the Electronic Properties of Thiol-protected gold nanoparticles," *Undergraduate Honors Thesis at The Pennsylvania State University*.

[24] Kang, H., J. T. Buchman, R. S. Rodriguez, H. L. Ring, J. He, K. C. Bantz, and C. L. Haynes (2019) "Stabilization of Silver and Gold Nanoparticles: Preservation and Improvement of Plasmonic Functionalities," *Chemical Reviews*, **119**(1), pp. 664–699.

[25] Hernandez, V. A. (2023) "An overview of surface forces and the DLVO theory," *ChemTexts*, **9**(10).

[26] Friedlein, J. T., R. R. McLeod, and J. Rivnay (2018) "Device physics of organic electrochemical transistors," *Organic Electronics*, **63**, pp. 398–414.

[27] Lee, H. J., J. H. Mun, I. H. Oh, K. Beom, T. S. Yoon, A. R. Hong, H. S. Jang, and D. H. Kim (2021) "Enhanced photodetector performance in gold nanoparticle decorated ZnO microrods," *Materials Characterization*, **171**.

[28] Ghittorelli, M., A. Adami, P. Romele, F. Giacomozzi, L. Lorenzelli, and F. Torricelli (2019) "ON-OFF current ratio in Organic Ferroelectric Memory Diodes: the role of the Density of States," *2019 IEEE International Conference on Flexible and Printable Sensors and Systems (FLEPS)*.

[29] Sufyan, S. A., B. van Devener, P. Perex, and M. M. Nigra (2023) "Electronic Tuning of Gold Nanoparticle Active Sites for Reduction Catalysis," *ACS Applied Materials & Interfaces*, **15**(1), pp. 1210–1218.

[30] Schubert, M. M., S. Hackenberg, A. C. van Veen, M. Muhler, V. Plzak, and R. J. Behm (2001) "CO Oxidation over Supported Gold Catalysts—"Inert" and "Active" Support Materials and Their Role for the Oxygen Supply during Reaction," *Journal of Catalysis*, **197**(1), pp. 113–122.

[31] Kong, F. Y., J. W. Zhang, R. F. Li, Z. X. Wang, W. J. Wang, and W. Wang (2017) "Unique Roles of Gold Nanoparticles in Drug Delivery, Targeting and Imaging Applications," *Molecules*, **22**(9).

[32] Fagan, J. W. and B. J. Lear (2020) "Dependence of Core Electronics of Gold Nanoparticles on Ligand, Solvent, and Sample Preparation," *The Journal of Physical Chemistry C*, **124**(44), pp. 24435–24440.

[33] Farre, J. C. (2013) *Gold Nanoparticles as Drug Delivery Agents. Detoxifying the Chemotherapeutic Drug Cisplatin*, Ph.D. thesis, Universitat Autònoma de Barcelona.

[34] Marcus, Y. (1998) *The Properties of Solvents*, Wiley.

[35] Kasap, S. O. (2001) *Principles of Electronic Materials and Devices, Second Edition*, McGraw-Hill Higher Education.

[36] Liu, J., H. He, D. Xiao, S. Yin, W. Ji, S. Jiang, D. Luo, B. Wang, and Y. Liu (2018) "Recent Advances of Plasmonic Nanoparticles and their Applications," *Materials*, **11**(10).